Ti-2007 Science and Technology, edited by M. Ninomi, S. Akiyama, M. Ikeda, M. Hagiwara, K. Maruyama
The Japan Institute of Metals (2007)

Compositional Modification and Property Evaluation of Orthorhombic Ti_2AlNb-Based Alloys

M. Hagiwara[1], Y. Mao[1] and S. Emura[l]

[1]*National Institute for Materials Science, 1-2-1 Sengen, Tsukuba, Ibaraki 305-0047, Japan*

The Ti-Al-Nb intermetallic alloys have been receiving considerable attention as potential lightweight and high strength materials for high temperature application. In order to enhance the mechanical properties, particularly creep, of Ti_2AlNb-based alloys, the beta-phase stabilizing elements such as Fe, Mo, Cr, W and V were each substituted systematically for a portion of niobium in the Ti-22Al-27Nb system. The creep behaviors under 200~380MPa stress at 650~750°C and tensile properties at room and elevated temperatures were evaluated. Comparing with Ti-22Al-27Nb alloy, Mo+Fe- and W+Cr-modified alloys exhibited much better creep resistances and higher yield strength at elevated temperatures. The mechanism of creep enhancement was also discussed.

Keywords: *orthorhombic titanium alloy, compositional modification, microstructure, tensile strength, creep*

1. Introduction

Titanium intermetallic alloys, based on the ordered orthorhombic Ti_2AlNb phase (O phase)[1)], have received considerable attention as potential high temperature structural materials, since Ti_2AlNb-based alloys have a higher specific strength, greater fracture toughness and better workability than conventional intermetallic alloys, such as TiAl-based and Ti_3Al-based alloys[2)]. The typical alloy system of Ti_2AlNb-based alloys so far developed is a Ti-22Al-27Nb alloy, consisting primarily of the (O+B2) two-phase microstructure. This alloy is reported to have a good balance of tensile, creep and fracture toughness properties [3)]. However, the high temperature mechanical properties, particularly creep properties, of the orthorhombic Ti_2AlNb-based alloys must be improved before commercial applications are feasible [4)]. In the present study, to improve the creep behavior of Ti_2AlNb-based alloys, the beta (β)-phase stabilizing elements such as Fe, Mo, Cr, W and V were substituted systematically for a portion of Nb in the baseline Ti-22Al-27Nb alloy. The microstructures and creep behaviors of the compositional modified alloys are reported and discussed.

2. Guideline for Compositional Modification

The guideline governing the alloy modification is based on the fact that the total sum of the β phase stability from each β-stabilizing element in the modified alloy should correspond to that of a Ti-22Al-27Nb alloy. This guideline suggests that the phase diagram for the modified alloy needs to be the same or very similar to that of a Ti-22Al-27Nb alloy, and, therefore, the same phase constitutions may be obtained with the same heat treatment applied to both modified and baseline alloys. Figure 1 shows the critical concentration of various β-stabilizers in titanium necessary to obtain a 100 % β phase at room temperature [5)] indicating that the β phase stabilizing ability becomes strong in the order of Fe, Mo, Cr, W, V and Nb. For example, Mo is Nb (22.5) / Mo (5.3) = 4.25 times stronger than that of Nb. It is reasonable therefore to assume that one atomic percent addition of Mo corresponds to the replacement of the 4.25 atomic percent of Nb. Similarly, one atomic percent addition of Fe corresponds to the replacement of the Nb (22.5)/ Fe (3.0)=7.5 atomic percent of Nb. By following this guideline, various modified alloys were produced as: Ti-22Al-19.2Nb-2Cr, Ti-22Al-12.5Nb-2W-2Cr, Ti-22Al-10.8Nb-2Mo-2Cr, Ti-22Al-16Nb-2Cr-2V, Ti-22Al-11Nb-2Mo-lFe and Ti-22Al-16.3 Nb-2V-1Fe.

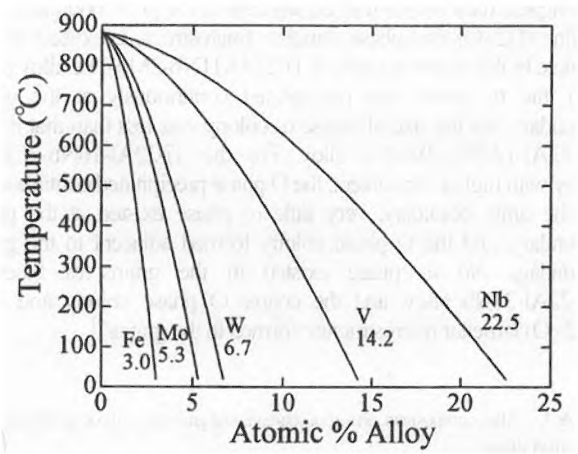

Figure 1. Ti-based binary phase diagram [5)].

3. Experimental

The alloy ingots were prepared by plasma arc melting. Each ingot, with a diameter of 46 mm, was encapsulated in an evacuated stainless steel can and hot rolled into 12 mm square bars at 1100°C in the single B2 phase region. After the hot processing, the alloys were annealed at 1100°C for 1 h and then cooled at a controlled cooling rate of 0.03 K/sec to produce a lamellar microstructure. Finally, the alloys were held at 800°C for 100 h in the (O+B2) two-phase region to stabilize the microstructure. The creep testing specimen had a 4.0 mm diameter and a 25 mm effective gauge length. Creep tests were conducted in air under a constant tensile load, using a dead-weight creep-rupture machine. The phase constitutions of the alloys were identified by the X ray diffraction (XRD) patterns. The microstructures were investigated with optical microscopy and scanning electron microscopy (SEM).

4. Results and Discussion

4.1 Microstructures

The XRD patterns showed that, after being heated at 1100°C for

1 h and then water-quenched, all of the alloys showed a single B2 phase structure. The grain sizes of the B2 phase were close to each other for these modified alloys (from 162 μm for Ti-22Al-16Nb-2Cr-2V to 195 μm for Ti-22Al-16.3Nb-2V-1Fe). The B2 phase grains along the rolling direction were elongated slightly, to 1.4 times the length in the transverse direction. During the further controlled cooling at a rate of 0.03 K/sec, the O and/or α_2 phases precipitated from the previously single B2 phase. The phase constitutions of the compositional modified alloys, after controlled cooling and annealing at 800°C for 100 h, were identified by XRD patterns and are summarized in Table 1. The density of each alloy is also listed in Table 1. The phase constitutions were (B2+O) phases for Ti-22Al-19.2Nb-2Cr, Ti-22Al-16Nb-2Cr-2V, Ti-22Al-16.3Nb-2V-1Fe and Ti-22Al-27Nb baseline alloys with higher Nb content, whereas the phase constitutions were (B2+O+α_2) phases for Ti-22Al-10.8Nb-2Mo-2Cr, Ti-22Al-11Nb-2Mo-1Fe and Ti-22Al-12.5Nb-2W-2Cr alloys with lower Nb content.

As typical examples, the microstructures of Ti-22Al-12.5Nb-2W-2Cr and Ti-22Al-11Nb-2Mo-1Fe alloys after controlled cooling and annealing are shown in Figure 2. The volume fractions and morphologies of the constitution phases in these alloys were a little different, depending on the alloy compositions. For the Ti-22Al-12.5Nb-2W-2Cr alloy (Fig. 2a) , the α_2 phase precipitated continuously at the B2 phase grain boundary, a coarse α_2 colony (elongated dark phase) formed adjacent to the grain boundary and a fine (B2+O) two-phase lamellar microstructure existed in the grains. In the microstructure of Ti-22Al-11Nb-2Mo-1Fe alloy (Fig. 2b), the α_2 phase also precipitated continuously at the grain boundary, but the size of coarse α_2 colony was less than that in the Ti-22Al-12.5Nb-2W-2Cr alloy. For the Ti-22Al-16Nb-2Cr-2V alloy with higher Nb content, the O phase precipitated continuously at the grain boundary, very little α_2 phase existed at the grain boundary and the O phase colony formed adjacent to the grain boundary. No α_2 phase existed in the grains of baseline Ti-22Al-27Nb alloy, and the coarse O phase colony and fine (B2+O) lamellar microstructure formed in the grains[6].

Table 1. Alloy composition, phase constitutions and grain sizes of compositional modified alloys.

Alloy	Density (g/cm^3)	Phase constitution
Ti-22Al-19.2Nb-2Cr	5.05	B2+O
Ti-22Al-12.5Nb-2W-2Cr	5.02	B2+O+α_2
Ti-22Al-10.8Nb-2Mo-2Cr	4.89	B2+O+α_2
Ti-22Al-16Nb-2Cr-2V	4.96	B2+O
Ti-22Al-11Nb-2Mo-1Fe	4.87	B2+O+α_2
Ti-22Al-16.3Nb-2V-1Fe	4.98	B2+O
Ti-22Al-27Nb	5.35	B2+O

4.2 Creep Behavior

The creep tests were conducted at 650◦C under a tensile load of 310 MPa and at 650 to 750◦C under a tensile load of 200 MPa. The creep strains vs. time curves under 650◦C/310 MPa conditions of the compositional modified alloys and the baseline Ti-22Al-27Nb alloy are shown in Figure 3. The creep curve is comprised of three normal creep stages: primary transient creep, steady-state creep and accelerating creep. From these creep curves, it is seen that the Mo+Fe- and W+Cr-modified alloys exhibited good creep resistance. The minimum creep rates were much lower than those

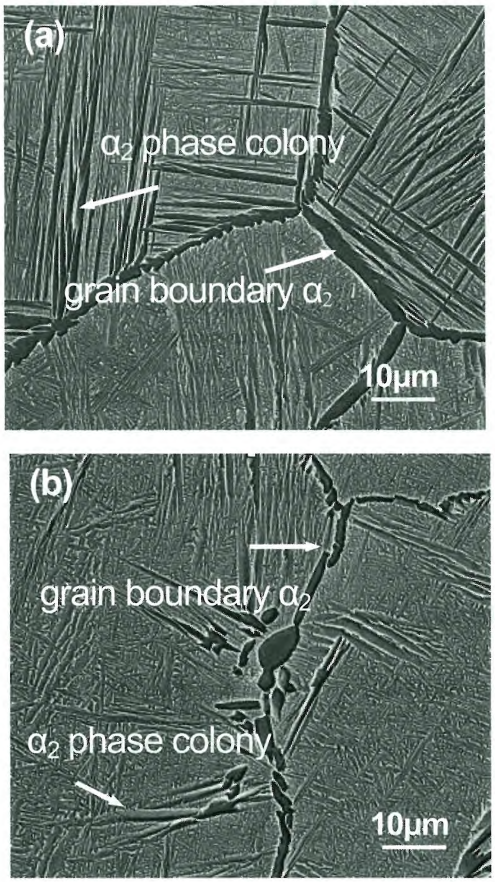

Figure 2. Microstructures of the compositional modified alloys after 1100 °C/1h, 0.03 K/sec controlled cooling and 800°C/100h. (a) Ti-22Al-12.5Nb-2W-2Cr and (b) Ti-22Al-11Nb-2Mo-1Fe.

of other modified alloys or of the Ti-22Al-27Nb alloy.

The creep behaviors of the modified alloys under 650°C/310 MPa and 650 to 750◦C/200 MPa conditions are summarized in Table 2. The transient creep time (ttr) is defined as the ending time of transient creep, and the transient creep strain (εtr) is determined by extrapolating the steady-state creep line to zero time. The 1% creep-strain life time under 650◦C/310 MPa condition was prolonged greatly in the Mo+Fe- modified alloy; it was 5.6 times that of Ti-22Al-27Nb alloy. The minimum creep rate of Mo+Fe-modified alloy was 3.1 times less than that of Ti-22Al-27Nb alloy. The transient creep strain of Mo+Fe-modified alloy was also much lower than that of Ti-22Al-27Nb alloy. The data of creep behaviors at 650 to 750◦C/200 MPa stress of Mo+Fe-, W+Cr-modified alloys and Ti-22Al-27Nb alloy also revealed that the minimum creep rate, the 1% creep-strain life time and the transient creep strain of Mo+Fe- modified alloy were all much better than the Ti-22Al-27Nb alloy under these conditions.

The temperature dependences of minimum creep rate for a 200 MPa tensile load are shown in Figure 4. The minimum creep rate follows the power-law creep equation, $\dot{\varepsilon}_{min} = A\sigma^n \exp(-Q_{app}/RT)$, where σ is the tensile stress, A and n are constants, Q_{app} is the apparent activation energy of the creep, R is the gas constant, and T is the absolute temperature. According to the above power-law equation, the values of Q_{app} were calculated from the slope of ln $\dot{\varepsilon}_{min}$ vs. 1/T plots. The values of Q_{app} for Mo+Fe- and W+Cr-modified alloys are 424 and 443 kJ/mol, respectively, which are much higher than the 278 kJ/mol of the Ti-22Al-27Nb alloy.

Table 2. Creep behaviors of the modified alloys under 650°C/310 MPa and 650 to 750°C/200 MPa creep condition

Creep condition/Alloy	Transient Creep Strain, εtr (%)	Transient Creep Time, ttr (h)	Minimum Creep Rate, $\dot{\varepsilon}_{min}$ (%/h)	1% Creep-Strain Life time (h)
650°C/310MPa				
Ti-22Al-19.2Nb-2Cr	0.51	10	5.80×10^{-2}	9
Ti-22Al-12.5Nb-2Cr-2W	0.90	500	2.08×10^{-3}	150
Ti-22Al-10.8Nb-2Cr-2Mo	0.73	30	2.56×10^{-2}	12
Ti-22Al-16.0Nb-2Cr-2V	0.40	28	2.54×10^{-2}	22
Ti-22Al-11.0Nb-2Mo-1Fe	0.35	600	1.58×10^{-3}	420
Ti-22Al-16.3Nb-2V-1Fe	0.48	4	1.41×10^{-1}	4
Ti-22Al-27Nb	0.72	300	5.88×10^{-3}	75
650°C/200MPa				
Ti-22Al-12.5Nb-2Cr-2W	0.74	750	4.10×10^{-4}	700
Ti-22Al-11.0Nb-2Mo-1Fe	0.49	800	3.32×10^{-4}	1550
Ti-22Al-27Nb	0.40	250	1.42×10^{-3}	420
700°C/200MPa				
Ti-22Al-12.5Nb-2Cr-2W	1.42	560	3.75×10^{-3}	85
Ti-22Al-11.0Nb-2Mo-1Fe	0.32	100	4.06×10^{-3}	160
Ti-22Al-27Nb	0.75	280	5.00×10^{-3}	95
750°C/200MPa				
Ti-22Al-12.5Nb-2Cr-2W	0.40	5	1.18×10^{-1}	5
Ti-22Al-11.0Nb-2Mo-1Fe	0.27	6	6.11×10^{-2}	13
Ti-22Al-27Nb	0.24	8	5.56×10^{-2}	13

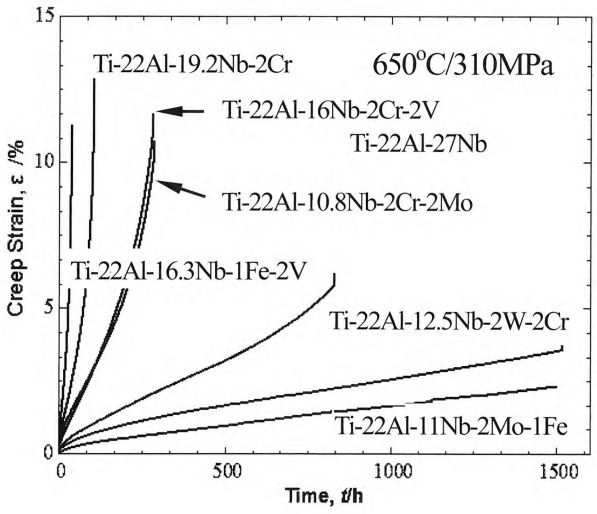

Figure 3. The creep strains vs. time curves under 650°C/310 MPa creep test

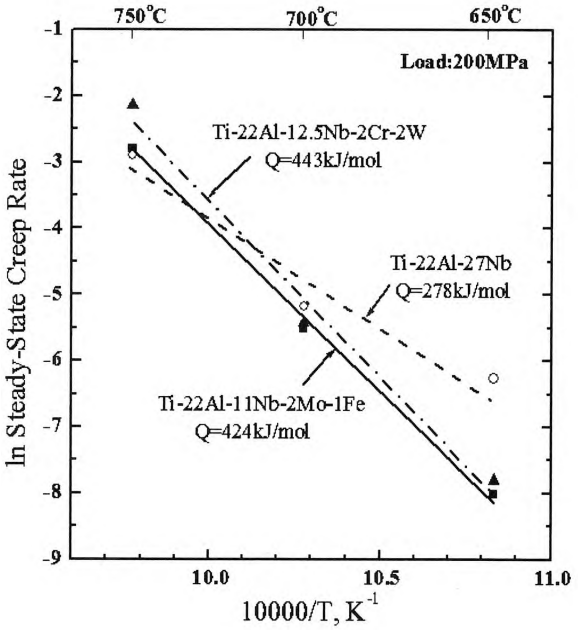

Figure 4. Temperature dependence of $\dot{\varepsilon}_{min}$ under 200 MPa creep test

For intermediate and high creep stresses (>100 MPa) at intermediate temperatures (650°C to 760°C), the creep mechanism of grain boundary sliding and dislocation-controlled creep were summarized as the creep behavior of Ti_2AlNb-based alloys [7]. The values 424 and 443 kJ/mol of apparent creep active energy of Mo+Fe- and W+Cr-modified alloys corresponded to the dislocation-controlled creep [7], suggesting that the creep process is controlled by dislocation climb.

Figure 5 shows the crept microstructures of Ti-22Al-11Nb-2Mo-1Fe, Ti-22Al-19.2Nb-2Cr and Ti-22Al-27Nb alloys. These microstructures indicate that grain-boundary sliding and cracking were the main creep deformation mechanisms for the baseline Ti-22Al-27Nb alloy (Fig. 5a), resulting in a medium minimum creep rate. For a Ti-22Al-19.2Nb-2Cr alloy with low creep resistance (Fig. 5b), the main creep deformation mechanisms were the phase-interface sliding and cracking, and also the grain-boundary sliding and cracking. In the crept microstructures of Mo+Fe- and W+Cr-modified alloys such as Ti-22Al-11Nb-2Mo-1Fe alloy (Fig. 5c), no grain-boundary sliding or cracking was observed. This result indicates again that the dislocation-controlled creep was the creep mechanism for the Mo+Fe- and W+Cr-modified alloys.

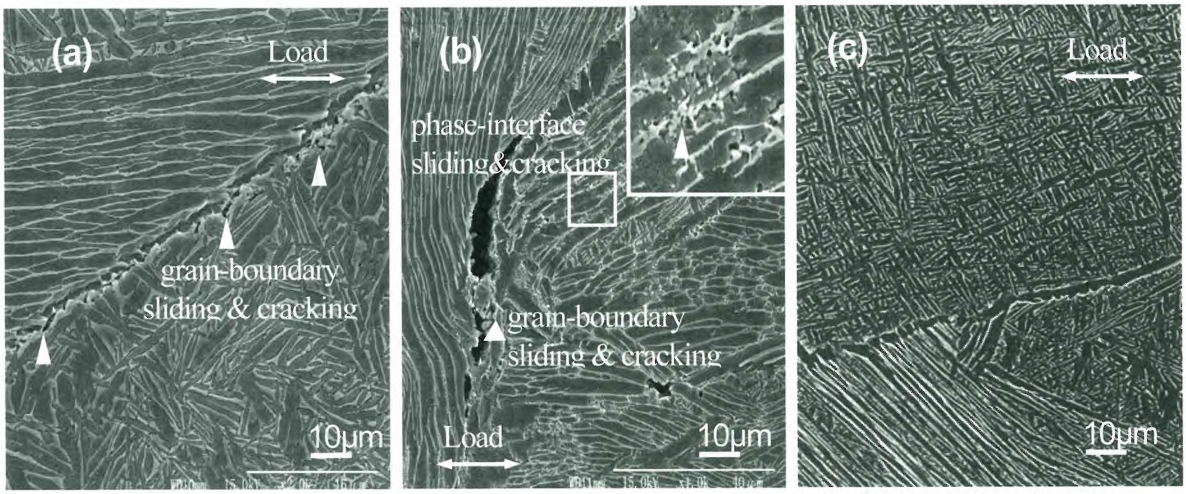

Figure 5. The crept microstructures under 650°C/310 MPa creep conditions in air. (a) Ti-22Al-27Nb, (b) Ti-22Al-19.2Nb-2Cr and (c) Ti-22Al-11Nb-2Mo-1Fe

5. Conclusions

β-phase stabilizing elements such as Fe, Mo, Cr, W or V were each substituted systematically for a portion of Nb in a Ti-22Al-27Nb alloy system. Six compositional modified alloys were created. The phase constitutions were found to be B2+O or B2+O+α_2 phases, depending on the alloy composition. The microstructures and creep behaviors were investigated under 650◦C/310 MPa and 650 to 750◦C/200 MPa conditions. Mo+Fe-modified alloys exhibited good creep resistance. The minimum creep rate, 1% creep-strain lifetime and transient creep behavior of Ti-22Al-11Nb-2Mo-1Fe alloy in the temperature range of 650 to 700◦C were better than those of Ti-22Al-27Nb alloy. The dislocation-controlled creep mechanism was suggested to be the creep mechanism for the Mo+Fe- and W+Cr-modified alloys.

RERERENCES

1) D. Banerjee et al: Acta Metall. 36 (1988), pp.871-882.

2)A. K. Gogia et al: Intermetallics. 6 (1998), pp.741-748.

3) R G Rowe: *Microstructure/Properties Relationships in Titanium Aluminides and Alloys*, ed by (TMS, Warrendale PA, USA 1991), pp.387-389.

4) F. Tang, S. Nakazawa and M. Hagiwara: Mater. Sci. Eng. A329 (2002), pp.492-.

5) S. Ankem and S. R. Seagle: *Beta Titanium Alloys in the 1980s*, ed. By R. R. Boyer, H. W Rosenberg, (TMS, Warrendale PA, 1983), pp.107-126.

6) M. Hagiwara, A. Araoka S.J. Yang, S. Emura and S. W. Nam: Metall. Mater. Trans. 35A (2004), pp.2161-2170.

7) C. J. Boehlert and D. B. Miracle: Metall. Mater. Trans. 30A (1999), pp.2349-2367.